TOPICS IN UPSILON SPECTROSCOPY AND B PHYSICS WITH CUSB

P. M. Tuts
S.U.N.Y. at Stony Brook
Stony Brook, NY
U.S.A.

ABSTRACT

We discuss some recent results in Υ spectroscopy and B meson physics from the CUSB collaboration at CESR. In particular, the recent observation of the $\chi_b(1^3P_J)$ state at (9901±3) MeV in both the inclusive, $(\Upsilon(2S)\to\gamma\chi_b)$, and exclusive, $(\Upsilon(2S)\to\gamma\chi_b\to\gamma\gamma\Upsilon(1S))$, photon spectra. Splittings and branching ratios are given. Results on the search for $\Upsilon'''\to B^*B$, limits on the B meson mass, and the relative couplings strengths for b quark decay are also given.

1.0 INTRODUCTION

The Υ system, which consists of a bound b quark and its antiquark, has proved to be a very rich testing ground for the study of b quarks, in terms of both their decay properties, and the forces that bind them (for a review of Υ physics see Ref. 1). The experimental study[2] of the Υ system at CESR has progressed extremely rapidly, from the observation[3] of the Υ, Υ' Υ'', and Υ''' states in 1980, to the observation by CUSB[4] of the χ_b' in 1982, and the χ_b in[5] 1983. In this paper we will discuss the CUSB results on the observation of the χ_b states from Υ' decays together with a summary of some of our results on B physics from recent running on the Υ''' as well as some other selected results from CUSB[6]. The Υ system spectrum is a very rich one, see Figure 1, with three bound triplet S states and one quasi-bound state just above the b flavor threshold; the P wave states are experimentally accessible through electric dipole (E1) transitions from the $\Upsilon'(2^3S_1)$ and $\Upsilon''(3^3S_1)$ states.

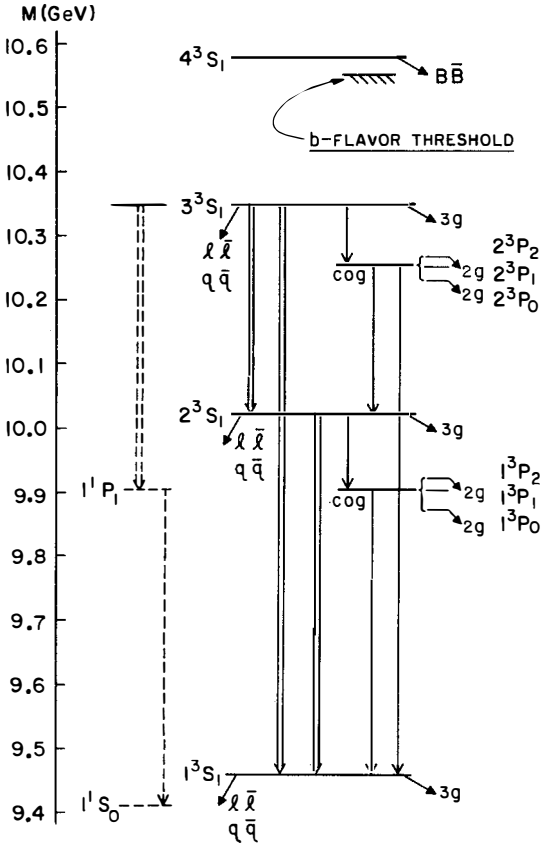

Figure 1. The bound $\Upsilon(b\bar{b})$ spectrum. The single and double lines indicate experimentally observed γ and $\pi\pi$ transitions respectively. The dashed lines indicate transitions that have not yet been observed.

2.0 THE CUSB DETECTOR

The CUSB detector, which is shown in perspective in Figure 2, is a high resolution segmented NaI and lead glass calorimeter. The innermost portion consists of four planes of tracking chambers, which are followed by ~9 radiation lengths of NaI crystals (324), ~7 radiation lengths of lead glass blocks (256), and NaI end caps (168). Intersperced between the five NaI layers

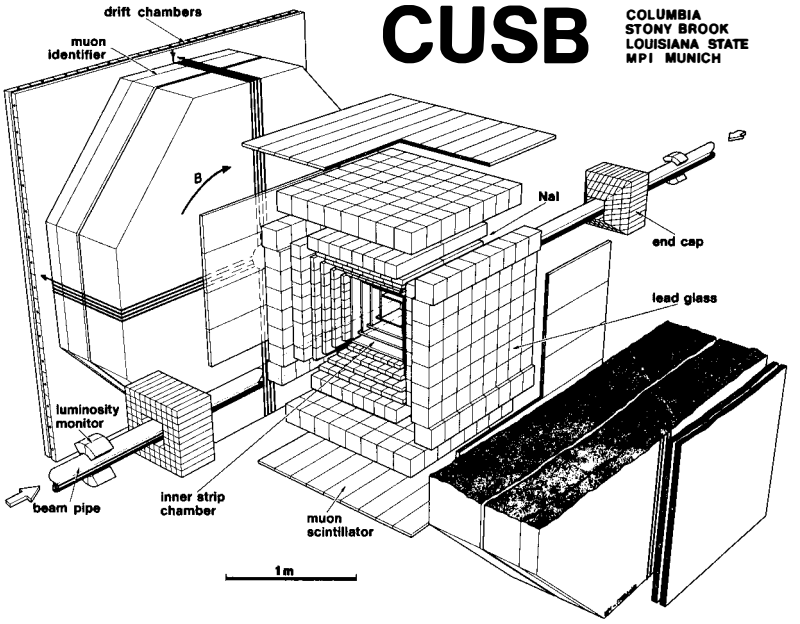

Figure 2. Perspective view of the CUSB detector, with the main detection elements listed. The end caps are shown pulled out for ease of display. The chambers between the NaI layers are not shown.

were additional tracking chambers; these chambers were removed for the most recent Υ' running in an effort to improve the resolution of the central detector from $\sigma_E/E \sim 4\%/E^{1/4}$ (E in GeV). Outside the lead glass array there is a scintillator hodoscope which provides us with a two muon trigger (in addition, horizontally moving muons pass through an iron muon identifier system). The solid angles are ~80%, and ~36% of 4π for back to back electrons, and muon pairs respectively. The relative energy calibration of all the NaI crystals is maintained by continuosly monitoring the positions of the photon lines from ^{137}Cs(.66 MeV) and ^{60}Co(1.17,1.33 MeV) sources which are mounted on the NaI crystals. This monitoring takes place simultaneously with data taking, allowing for continuous gain monitoring of the entire system. The lead glass calibration is maintained through daily monitoring of LED light sources placed on the blocks. The energy calibration obtained in this manner is then corrected for Monte Carlo calculated losses in the inactive material between crystals. The final energy calibration is then checked against summed photon energies from exclusive photon events and Bhabha scattering events; it differs by only a few percent.

3.0 Υ SPECTROSCOPY

3.1 The N^3S_1 States

The agreement of the measured leptonic widths and masses of the four Υ states observed in R (shown in Figure 1 of Ref. 7) with potential models[2] has lead to the association of these states with the first four triplet S states of the $b\bar{b}$ system. The values are summarised in Table I where masses are scaled to $M(\Upsilon)$=9460 MeV as measured[8] at VEPP-4. Note that the $\Upsilon(4^3S_1)$ state lies above the b flavor threshold since the observed[3] width is significantly wider than the measured machine resolution, providing us with a B factory with which to study B decay.

3.2 Search For Other States

Besides the four prominent resonances that have been observed in the e^+e^- cross section, we have searched for others in the continuum regions between the various resonances. The scans and the results are shown in Figures 3a,b,c for the regions below the Υ', below the Υ'' and between the Υ'' and the Υ''' respectively. The most thorough scanning was carried out in the latter region, where there is a prediction[9] for the lowest lying vibrational state, having a leptonic width of 70-270 eV.

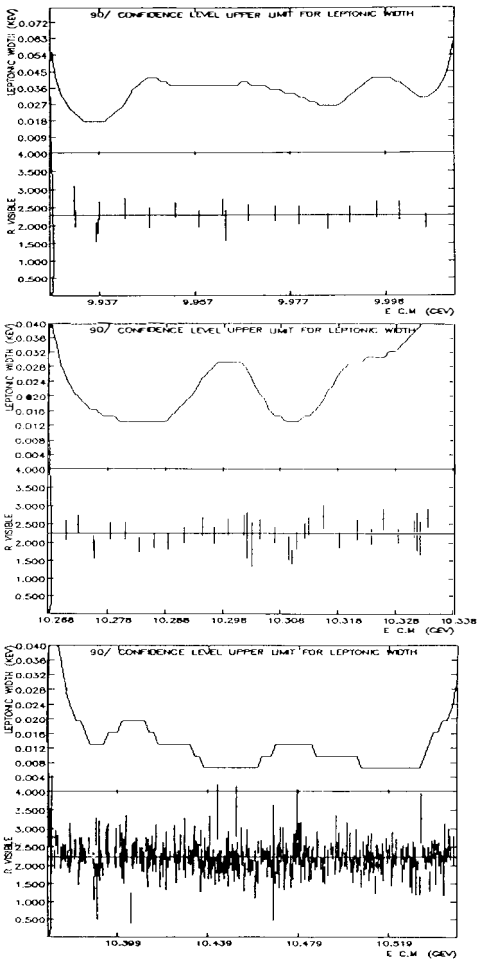

Figure 3. The 90% CL upper limit leptonic width in KeV for narrow resonances (top), and the scan data points in R for the energy regions: (a) $9.93<M<10.01$ GeV/c^2, (b) $10.27<M<10.335$ GeV/c^2, (c) $10.37<M<10.55$ GeV/c^2.

There is no evidence for any narrow states (i.e. of machine resolution) in any of the regions. In particular, a vibrational state with leptonic width greater than 20 eV is excluded, in conflict with vibrational state predictions.

Table I. The masses and leptonic widths for the ^3S states of the Υ system. The Υ mass is from Ref. 8. The theoretical predictions are from Ref. 2, with the leptonic widths calculated using the Υ experimental value.

Resonance	-- Mass (MeV/c^2) --		Leptonic width (keV)	
	Experiment	Theory	Experiment	Theory
$\Upsilon(1^3S_1)$	9459.7	9459.7	1.14±0.05	1.05-1.07
$\Upsilon(2^3S_1)$	10020.5±0.7	10025	0.50±0.03	.44-.50
$\Upsilon(3^3S_1)$	10350.0±0.7	10322-10360	0.35±0.03	.31-.40
$\Upsilon(4^3S_1)$	10578.0±3.0	10568-10640	0.21±0.05	.25-.31

3.3 Decays Of The $\Upsilon''(3^3S_1)$

Since the CUSB results on the decays of the $\Upsilon(3S)$ have been discussed elsewhere[4] and in the Moriond Workshop proceedings[7], we will limit ourselves here to a brief summary of those results. The most significant discovery made was the observation of the χ_b' (or $2^3P_{J=0,1,2}$) state in both the inclusive photon spectrum, $\Upsilon(3S)\to\gamma+X$, and the exclusive decay chain $\Upsilon(3S)\to\gamma+\chi_b'$, $\chi_b'\to\gamma+(\Upsilon(2S)$ or $\Upsilon(1S))$ with the final S state decaying to e^+e^- or $\mu^+\mu^-$. The results were obtained from a sample of ~65 000 hadronic events on the $\Upsilon(3S)$ peak, and are summarised (together with the results from $\Upsilon(2S)$ decays) in Table III. In addition, the $\pi^+\pi^-$ hadronic transitions from the $\Upsilon(3S)$ to the $\Upsilon(2S)$ and $\Upsilon(1S)$ have been measured[10] and are summarised in Table II.

Table II. The hadronic $\pi\pi$ transition branching ratios measured by CUSB (see Ref. 10). The theoretical predictions are from Ref. 11.

Transition	Branching Ratio (%)	
	Experiment	Theory
$\Upsilon'\to\chi\pi^+\pi^-$	18±6	17-18
$\Upsilon''\to\Upsilon'\pi^+\pi^-$	3.1±2.0	1.5-2.3
$\Upsilon''\to\chi\pi^+\pi^-$	3.9±1.3	1.4-3.4

3.4 Decays Of The $\Upsilon'(2^3S_1)$

3.4.1 Inclusive Photons -

Encouraged by the success of having discovered the χ_b' states in the decays of the $\Upsilon(3S)$, the CUSB group has spent the last running period at CESR (Dec 1982 - March 1983) studying the decays of the $\Upsilon(2S)$ with the hope of observing the χ_b state in E1 photon transitions. Such transitions have been observed in both the inclusive and exclusive photon spectra[5], and can be associated with the χ_b states ($1^3P_{J=0,1,2}$). During this run CESR delivered ~30 pb^{-1} of integrated luminosity, corresponding to ~230 000 hadronic events in CUSB, of which ~153 000 are observed $\Upsilon(2S)$ decays (or ~180 000 produced $\Upsilon(2S)$ events). The principal philosophy behind the photon algorithm for shower recognition from the transverse and longitudinal shower shape has not changed from the $\Upsilon(3S)$ analysis[4]. However, we have since increased the efficiency for hadronic event recognition by ~30%, and tightened the photon criteria so as to maintain a constant photon finding efficiency of 13% over the energy range from 80 to 500 MeV. In addition the resolution for showers was improved to $\sigma_E/E \sim 3.6\%/E^{1/4}$ (E in GeV), due in part to the removal of the chambers between the NaI layers. The inclusive photon spectrum from the $\Upsilon(2S)$ is shown in Figure 4a. There is evident structure at ~125 MeV which is not visible in the $\Upsilon(1S)$ or continuum spectra. The background curve is obtained from the spectrum by fitting the region from 65 to 280 MeV with a cubic plus 3 gaussians of arbitrary position and normalization (the width of each was held fixed at σ_E/E ~6%), and the remainder of the spectrum with polynomials (excluding two bins around 430 MeV, where we expect to see a signal). The cubic fit is also required to match the polynomial fits at the

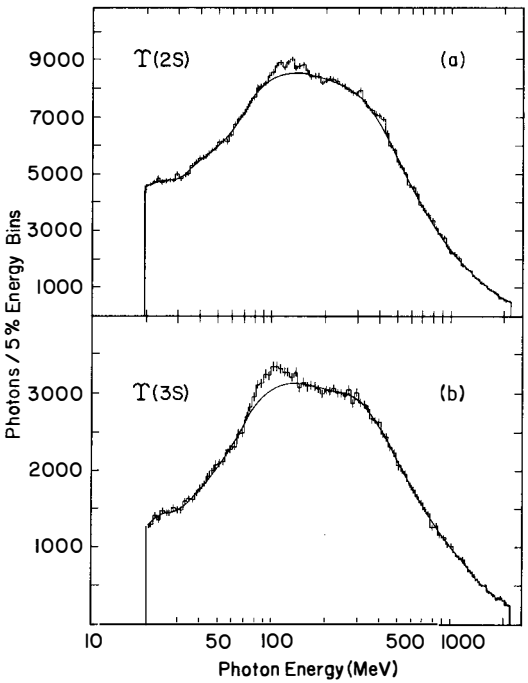

Figure 4. The inclusive photon spectra, $\Upsilon(nS) \rightarrow \gamma X$, for decays of (a) the $\Upsilon(2S)$, and (b) the $\Upsilon(3S)$. The solid line is the background, for details see text.

boundaries. The solid line shown in Figure 4a represents the cubic and polynomial terms alone. The contribution from the decay $\Upsilon(2S) \rightarrow \pi^0\pi^0\Upsilon(1S)$ (which has a BR~ 10%) is automatically taken into account because it contributes a smooth distribution from 20 to 420 MeV, peaking at 175 MeV on the plot. In addition, we show, in Figure 4b, the inclusive photon spectrum for decays of the $\Upsilon(3S)$ using both the new hadronic event and photon finding algorithm. We still see a distinct excess of photons in the 100 MeV region, leading to the the same positions and the same[4] $BR(\Upsilon(3S) \rightarrow \gamma + 2^3P_J) \sim 34\%$.

Returning to the $\Upsilon(2S)$ spectrum, we find a prominent excess in the region from 90 to 160 MeV (3110±323 counts) and another smaller excess in the region around ~427 MeV of 833±166 counts, as shown in

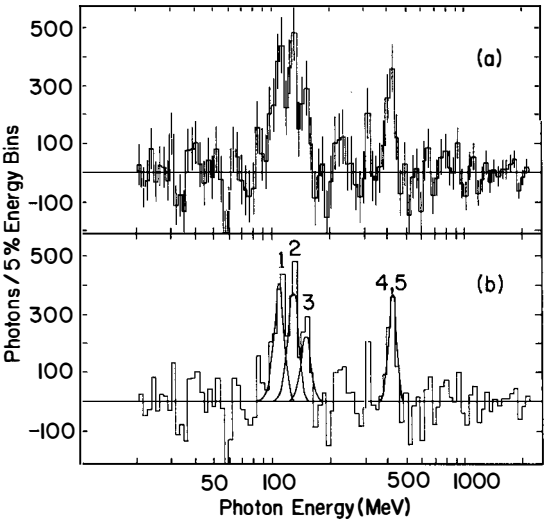

Figure 5. The background subtracted photon spectrum for $\Upsilon(2S) \rightarrow \gamma X$. The error bars are shown in (a), and (b) shows the fits to the excess. The numbers in (b) refer to Figure 6.

the subtracted spectrum of Figure 5a. The three gaussian fit to the excess at ~125 MeV yields photon line energies of 108, 128, and 149 MeV respectively. The individual gaussians are shown in Figure 5b superimposed on the subtracted spectrum, where the numbers refer to the photon lines indicated on Figure 6. Since the lines are more widely separated than in the 2^3P_J case and since our resolution is slightly improved, we are able to partially resolve the three photon lines as evidenced by figures 4a, and 5b. The final energy scale, after Monte Carlo correction for

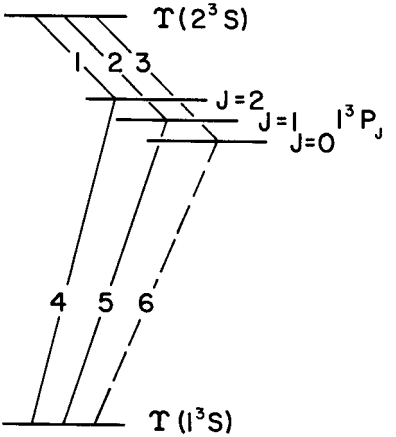

Figure 6. The E1 transitions for $\Upsilon(2S) \rightarrow \gamma\chi_b$ and $\chi_b \rightarrow \gamma\Upsilon(1S)$ decays. The dashed line indicates that this transition is suppressed.

energy loss in the inactive material, is determined by a sample of $\Upsilon(2S)\to\Upsilon(1S)\pi^0\pi^0\to\Upsilon(1S)+4\gamma$ events, where the summed 4γ energy (including $\Upsilon(1S)$ recoil) must add to $M(\Upsilon')-M(\Upsilon)$ ~561 MeV (as shown in Figure 7). This amounts to a 2% upward correction to the energy scale. If indeed these photons correspond to the E1 transitions to a P wave state, then one expects to see the 'mirror' transition from the P wave back down to the ground state, $\Upsilon(1S)$. The energy of the two photons (plus recoil energy of ~10.5 MeV) must therefore equal $M(\Upsilon(2S))- M(\Upsilon(1S))$. The product branching ratios for the three transitions via the P wave state are in the ratio of 2:5:~0 for the J=2,1,0 spin states respectively (as is shown in the following section on exclusive $\Upsilon(2S)$ decays). Thus from the measured inclusive photon lines we find that (108x2 + 128X5)/7 + 427 +10.5 ~560 MeV (including recoil) is precisely the M(2S)-M(1S) mass difference, from which we conclude that we have indeed seen the decay chain from the $\Upsilon(2S)$ to the $\Upsilon(1S)$ via an intermediate state that we associate with the χ_b. The photon excess observed in the 125 MeV region leads to a $BR(\Upsilon(2S)\to\gamma\chi_b)= (15.5\pm2.5)\%$ with an additional systematic uncertainty of +5% and −2.5%; if the excess at $(427\pm1\pm8)$ MeV is from the above decay chain, then we find the $BR(\Upsilon(2S)\to\gamma\chi_b)\times BR(\chi_b\to\gamma\Upsilon(1S))= (4\pm1)\%$. Using the above ratio of product BR's we find $BR(1^3P_2\to\gamma\Upsilon(1S))=(20\pm5)\%$, and $BR(1^3P_1\to\gamma\Upsilon(1S))=(47\pm18)\%$.

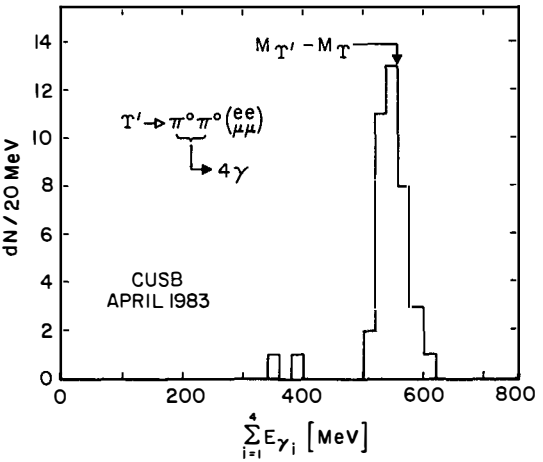

Figure 7. The total energy distribution for the four γ's from the hadronic decay $\Upsilon(2S)\to\pi^0\pi^0\Upsilon(1S)$, where $\Upsilon(1S)\to e^+e^-$ or $\mu^+\mu^-$.

The individual intensities of the three lines are consistent with those expected for E1 transitions (i.e. proportional to $k^3(2J+1)$, where k is the photon energy). After correction for that factor we find them to be 1.04 ± 0.3, 1, and 1.13 ± 0.5 for the J=2,1, and 0 states respectively, normalizing to the middle line. This evidence, together with the good agreement of the cog position with potential models, leads us to associate the observed lines with the lowest three triplet P wave states, $1^3P_{J=0,1,2}$. We summarise the inclusive photon results for the 1^3P_J and 2^3P_J states in Table III.

Table III. Summary of inclusive photon transitions. For potential model predictions, see Ref. 2.

Line	E_γ Energy (MeV)	-- Mass (MeV/c^2) -- Experiment	Theory	n	J	BR(Υ(nS)->γ(n-1)P_J) BR(%)	E1 width (keV) Expt.	Theory
2^3P_2	84.5±2.0±4	10265		3	2			
2^3P_1	99.5±3.2±4	10250		3	1			
2^3P_0	117.2±5.0±4	10232		3	0			
2Pcog	93.1±5	10256±5	10242-10271	all		34±3	8.4±1.4	4.8-7.6
1^3P_2	108.2±0.3±2	9912		2	2	6.1±1.4		
1^3P_1	128.1±0.4±3	9892		2	1	5.9±1.4		
1^3P_0	149.4±0.7±5	9870		2	0	3.5±1.4		
1Pcog	119.4±3	9900±3	9888-9924	all		15±2.5	4.9±1.0	3.1-4.4

3.4.2 Exclusive Photons -

In addition to the observation of the χ_bs in the inclusive spectrum, we have observed them in the exclusive events $\Upsilon(2S) \rightarrow \gamma\chi_b \rightarrow \gamma\gamma\Upsilon(1S) \rightarrow \gamma\gamma(e^+e^-$ or

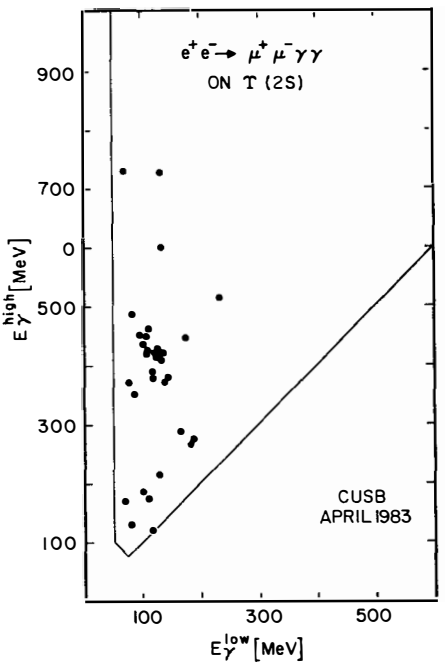

Figure 8. Scatter plot of γ energies for $\mu^+\mu^-$ final state cascade decays of the $\Upsilon(2S)$.

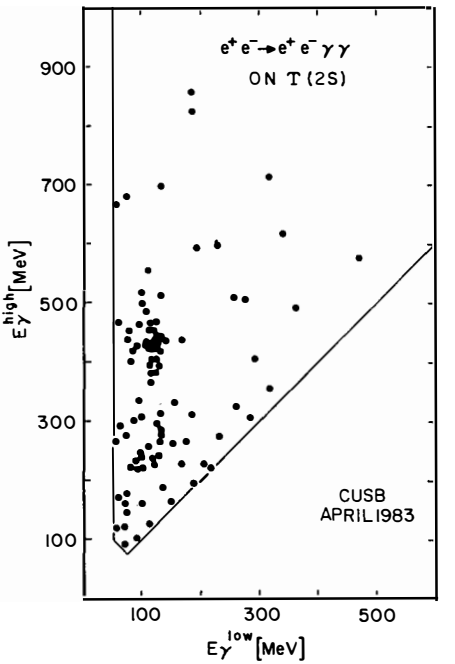

Figure 9. Scatter plot of γ energies e^+e^- final state cascade of the $\Upsilon(2S)$.

$\mu^+\mu^-$). Again, the proceedure is the same as that for the $\Upsilon(3S)$ exclusive events described elsewhere[4,7], except that the muon solid angle was increased to 36% of 4π. The acceptances for these exclusive events are 17% for events with e^+e^- final states and 12% for those with $\mu^+\mu^-$. The data are plotted in scatter plots of the two photon energies, E_γ^{low} vs E_γ^{high}, for electron and muon final state events separately in figures 8,9 respectively. Both plots show a distinct clustering at (E_γ^{low}, E_γ^{high}) ~ (120,430) MeV which we interpret as radiative cascade events via the χ_b. The fact that we are indeed observing cascade events to the $\Upsilon(1S)$ is well demonstrated in figure 10 which shows the sum of the two photon energies with a clear peak at the $\Upsilon(2S)$-$\Upsilon(1S)$ mass difference (after recoil correction).

The backgrounds are of interest only in the region of the clustering; hadronic cascade backgrounds via $\pi^o\pi^o$ are negligable above a summed energy of ~500 MeV. Other backgrounds for the $\mu^+\mu^-$ events are negligable (1±1 events), whereas for e^+e^- events there is a background from double radiative Bhabha events which is calculated to be 4±3 events in the region of

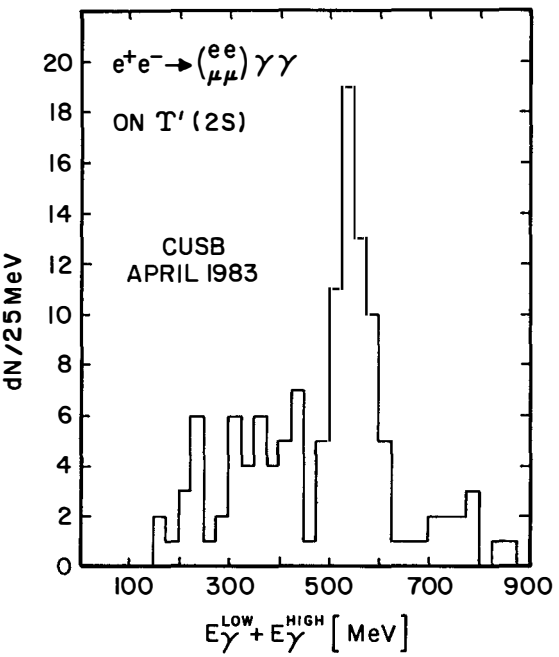

Figure 10. The summed photon energy for all the cascade events in Figures 8 and 9.

clustering of $80 < E_\gamma^{low} < 150$ MeV. The total observed number of events in that region is 51. Correcting for acceptance and background (together with a $B_{\mu\mu}$=.028 ±.003) we derive the product branching ratio $BR(\Upsilon(2S)\to\gamma\chi_b) \times BR(\chi_b\to\gamma\Upsilon(1S))$= (3.9±0.9)%. We have compared the splitting observed in these exclusive events with that obtained from the inclusive analysis, by combining both the e^+e^- and $\mu^+\mu^-$ data, constraining the $\gamma\gamma$ energy sum to 560 MeV (corrected for recoil and weighted by resolution) and fitting the low energy photon spectrum. The spectrum is shown in figure 11, where two clear peaks are visible; a two Gaussian fit (of equal widths) leads to fitted peak values of (106±3) MeV and (127±2) MeV with a resolution of σ_E/E= (4.5±0.7)%. The

fitted intensities are in the ratio of (.45±.19):1. The total product branching ratio, and intensity ratios, are in agreement with theoretical predictions (see Table IV), which leads us to make the association of these two lines with the 1^3P_2 and 1^3P_1 states. These results are summarised in Table IV.

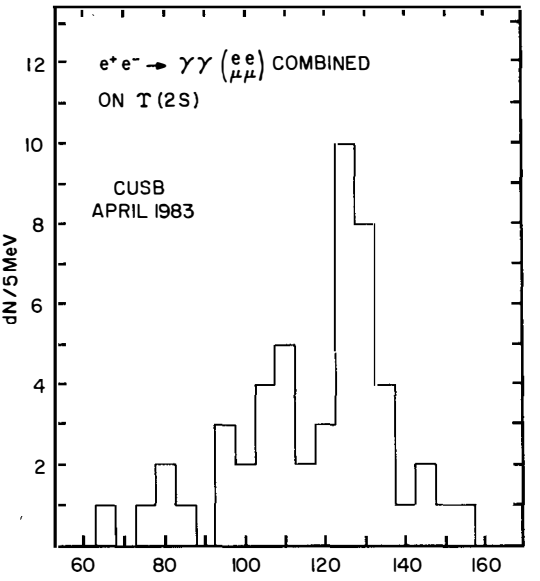

Figure 11. The projection of the low energy photon for Υ(2S) decays, showing peaks at 106 and 127 MeV.

Table IV. Summary of Υ(2S) and Υ(3S) exclusive events. E_γ^{LOW} (MeV)

Reaction	Branching Ratio (%) Experiment	Theory
$\sum_{j=1}^{3} BR(\Upsilon'' \to \gamma_j \chi'_{bj}) \times BR(\chi'_{bj} \to \gamma\Upsilon')$	5.9±2.1	3.3
$\sum_{j=1}^{3} BR(\Upsilon'' \to \gamma_j \chi'_{bj}) \times BR(\chi'_{bj} \to \gamma\Upsilon)$	3.6±1.2	2.8
$\sum_{j=1}^{3} BR(\Upsilon'' \to \gamma_j \chi_{bj}) \times BR(\chi_{bj} \to \gamma\Upsilon')$	<3.0	1.1
$BR(\Upsilon' \to \gamma_j \chi_{b2}) \times BR(\chi_{b2} \to \gamma\Upsilon)$	1.3±.7	3.3±.3
$BR(\Upsilon' \to \gamma_j \chi_{b1}) \times BR(\chi_{b1} \to \gamma\Upsilon)$	2.6±.8	
$BR(\Upsilon' \to \gamma_j \chi_{b0}) \times BR(\chi_{b0} \to \gamma\Upsilon)$	<.4	

4.0 B PHYSICS

In this section we present a brief summary of some of the recent results obtained by CUSB in the area of B physics. For more details on the CUSB B physics see Ref. 7.

4.1 Search For B*'s

In a sample of 39 000 Υ(4S) events, we have searched for the decay Υ(4S)→ B^*B, where the $B^* \to \gamma B$. The energy of the γ is expected to be ~50 MeV from scaling arguments. We do not observe any events in the inclusive photon spectrum of Υ(4S) decays[12], as shown in Figure 12. The shaded region in the figure indicates the expected signal if there were one photon per event. A

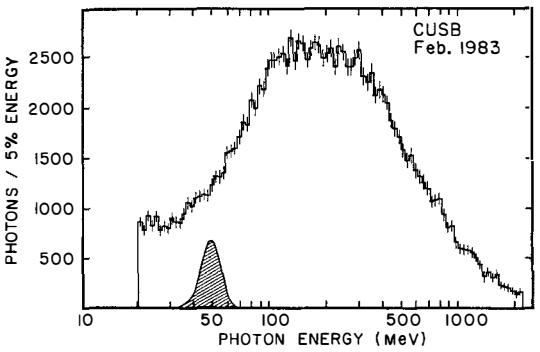

Figure 12. The continuum subtracted inclusive photon spectrum, $\Upsilon(4S) \rightarrow \gamma X$. The shaded curve represents the expected photon signal if there were one 50 MeV γ per event.

maximum likelihood analysis yields an upper limit on $BR(\Upsilon(4S) \rightarrow B^*B) < 7\%$ (90% CL) for $40 < E_\gamma < 60$ MeV. From these results and the measured width of the $\Upsilon(4S)$, we calculate[12] that $5263 < M_B < 5278$ MeV, in good agreement with the recently obtained CLEO value[13].

4.2 Electron Spectrum From B Decay

We have measured the electron spectrum (>1GeV electrons) for B decays on the $\Upsilon(4S)$. The experimental spectrum is shown in Figure

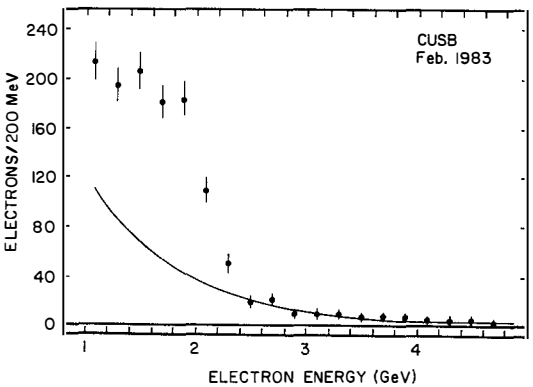

Figure 13. The measured electron spectrum (E_e> 1GeV) for $\Upsilon(4S)$ decays. The solid line is the measured background off resonance.

13, where the solid line is a fit to the measured continuum spectrum taken off the $\Upsilon(4S)$ peak. The continuum spectrum comes from electrons from D decay (recall that only ~30% of the events at the Υ''' energy are resonance events). The efficiency for >1 GeV electrons is ~7% (due to 20% electron identification and 34% solid angle). We observe 711 ± 47 events (after subtraction of 114 events from γ conversions and hadronic interactions) which leads to a $BR(B \rightarrow e\nu X) = (13.7 \pm 0.9 \pm 2)\%$. The above branching ratio was obtained assuming that 88% of electrons from $B \rightarrow e\nu X$ decay are above 1 GeV, and a 12% background contribution from $B \rightarrow DX$ decays.

The shape of the electron spectrum has been used to determine the ratio of contributions from b->u vs b->c, by comparison with the calculations of Altarelli et al[14]. The three curves in Figure 14 represent the expected spectra for the cases that m_q=1.8 GeV/c^2 (curve B), or that m_q=150 MeV/c^2 (curve A), and the contribution from B-> DX decay (curve C). A maximum likelihood calculation results in a spectrum consistent with no b->u contribution, the 90% CL limit leads to $BR(B\to e\nu X_u)/BR(B\to e\nu X_c) < 7\%$ or in terms of the coupling parameters of the mixing matrix $|V_{bu}/V_{bc}|^2 < .03$ (for details see Ref. 7).

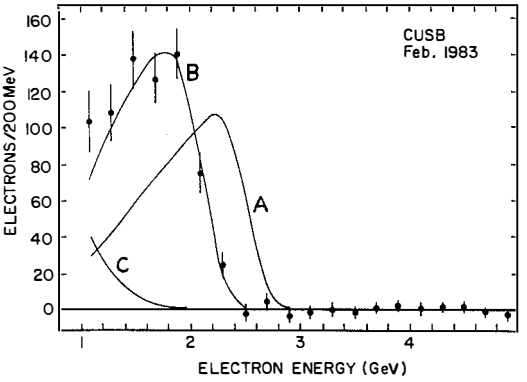

Figure 14. The subtracted electron spectrum on the $\Upsilon(4S)$. The curves are: (A) complete b->u, (B) complete b->c, and (C) electrons from D decay.

5.0 CONCLUSIONS

The Υ system has provided an amazing laboratory for the study of both weak and strong interactions. The Υ spectrum[2] has filled out experimentally in the last year with the addition of the χ_b and χ_b' members[4,5] to the Υ family, in support of the flavor independent potential model predictions for the bound $b\bar{b}$ system. The E1 rates are in agreement with theoretical expectations[5], and the hadronic transitions between triplet S states have been measured[10] and agree with those predicted by the QCD multipole expansion[11], although some of the spectra for these transitions are unexpected theoretically. In B physics, the B meson mass has been measured[12] and tight bounds have been placed on the quark mixing matrix parameters from the shape of the B decay electron spectrum[7]. Although much has been accomplished these past few years, there still remains the challenge of explicitely resolving the P wave lines, and observing the singlet S state, the η_b (see Figure 1). We hope to accomplish these tasks with the addition of a BGO upgrade[15] of the CUSB detector. The first quadrant of BGO should be installed and running by the end of 1983 (the η_b must await a full cylinder of BGO), and perhaps by the next Moriond meeting we will be able to report on yet more exciting results.

6.0 ACKNOWLEDGEMENTS

The author wishes to acknowledge the US National Science Foundation for his research support. Thanks must go to Juliet Lee-Franzini, Paolo Franzini, and Dean Schamberger for valuable discussions, and also to the CUSB collaboration. J. Tran Thanh Van and the organizers are to be congratulated for arranging a very stimulating conference.

7.0 REFERENCES

1. P.Franzini and J. Lee-Franzini, Phys. Rep. 81, 239(1982); P. Franzini and J. Lee-Franzini, Ann. Rev. Nucl. Part. Sci. 33, 1(1983).

2. For a detailed list of references see Ref. 1.

3. D. Andrews et al., Phys. Rev. Lett. 44, 1108(1980); ibid, 45, 219(1980); T. Böhringer et al., Phys. Rev. Lett. 44, 1111(1980); G. Finocchiaro et al., Phys. Rev. Lett. 45, 222(1980).

4. K. Han et al., Phys. Rev. Lett. 49, 1612(1982); G. Eigen et al., Phys. Rev. Lett. 49, 1616(1982).

5. C. Klopfenstein et al., submitted to Phys. Rev. Lett. (1983); F. Pauss et al., submitted to Phys. Rev. Lett. (1983).

6. The recent members of the CUSB collaboration include: P. Franzini, K. Han, D. Peterson, E. Rice, D. Son, J.K. Yoh, S. Youssef, T. Zhao (Columbia U.); J. Horstkotte, C. Klopfenstein, J. Lee-Franzini, R. D. Schamberger, M. Sivertz, L. J. Spencer, P. M. Tuts (SUNY, Stony Brook); H. Dietl, G. Eigen, E. Lorenz, G. Mageras, F. Pauss, H. Vogel (MPI, Munich); R. Imlay, G. Levman, W. Metcalf, V. Sreedhar (LSU); S. W. Herb (Cornell U.).

7. P. Franzini, in these proceedings.

8. A. S. Artamonov et al., Inst. of Nucl. Phys. Preprint 82-94 (1982).

9. W. Büchmuller and S.-H. H. Tye, Phys. Rev. Lett. D22, 594 (1980).

10. G. Mageras et al, Phys. Rev. Lett. 46, 1115 (1981); G.Mageras et al, Phys. Lett. 118B, 453 (1982).

11. Y.-P. Kuang and T.-M. Yan, Phys. Rev. D24, 2874 (1981).

12. R. D.Schamberger et al, Phys. Rev. Lett. D26, 720(1982).

13. E. Thorndike, in these proceedings.

14. G. Altarelli et al, Univ. of Rome Preprint 302 (1982).

15. P. M.Tuts and P. Franzini, Proceedings of the International Conference on Bismuth Germanate, edited by C. Newman-Holmes (Princeton University, Princeton, NJ, 1983) p596.